Available online at www.sciencedirect.com

ScienceDirect

journal homepage: www.elsevier.com/locate/he

Prediction of hydrogen-assisted fracture under coexistence of hydrogen-enhanced plasticity and decohesion

Song Huang [a,b], *Hu Hui* [a,*], *Jian Peng* [b]

[a] *School of Mechanical and Power Engineering, East China University of Science and Technology, Shanghai 200237, PR China*

[b] *Jiangsu Province Engineering Research Center of High-Level Energy and Power Equipment, Changzhou University, Jiangsu, PR China*

HIGHLIGHTS

- Competitive & Cooperative ductile-brittle damage model on HELP & HEDE interplay.
- Predicted Hydrogen embrittlement features match experimental observations.
- K_{JC} and K_{THa} prediction outputs match experiment values.
- Difference in hydrogen damage kinetics in different test methods captured.

GRAPHICAL ABSTRACT

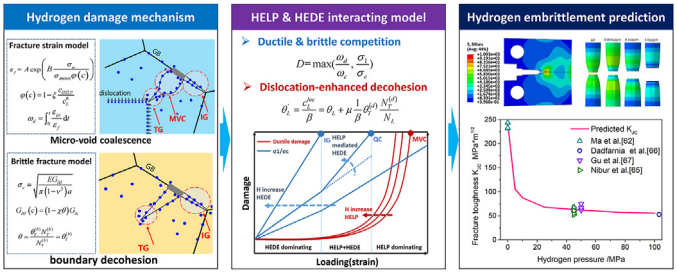

ARTICLE INFO

Article history:
Received 1 May 2023
Received in revised form
31 May 2023
Accepted 3 June 2023
Available online 24 June 2023

Keywords:
Hydrogen embrittlement
HELP+HEDE
HELP-mediated HEDE
Ductile to brittle transition
Numerical method

ABSTRACT

This work presents a novel strategy to model the coexistence of HELP & HEDE mechanisms. The proposed method accounts for ductile and brittle damage with a competitive fracture criterion to describe the competition effect between HELP & HEDE mechanisms. The cooperation aspect is addressed by a dislocation-enhanced hydrogen accumulation model, which agrees with the HELP-mediated HEDE mechanism. The tensile, fracture toughness, and threshold stress intensity factor tests are simulated in different hydrogen environments. The results demonstrate that the proposed method reproduces the hydrogen-dependent ductile to brittle transition phenomenon. Under different hydrogen conditions, the dominating damage mechanism and degradation trends agree with experimental observations. Furthermore, for the investigated 4130 steel, the predicted value of fracture toughness and threshold stress intensity factor match the experiment results. The difference in damage kinetics inherent in the two test methods is captured, which supports the rationality of the proposed strategy for HELP and HEDE interaction.

* *Corresponding author.*
E-mail address: huihu@ecust.edu.cn (H. Hui).

https://doi.org/10.1016/j.ijhydene.2023.06.033

Introduction

Hydrogen embrittlement (HE) is a primary threat to the safe operation of hydrogen storage equipment. Hydrogen, mainly pressurized gaseous hydrogen, is detrimental to most engineering materials [1–3]. HE provokes ductility and fatigue resistance loss, compromises the structural integrity, and leads to catastrophic brittle rupture. Therefore, the structural design of hydrogen storage equipment must include the influence of HE. In this regard, predicting hydrogen-assisted fracture is an essential engineering design requirement. However, most of the existing HE prediction techniques only emphasize the dominance of some specific HE mechanisms, which differs from the actual situation where multiple hydrogen embrittlement mechanisms could coexist. The Gap between the knowledge and the actual HE behavior leads to unreliable prediction and assessment of hydrogen-assisted fracture, which rises the potential risk of hydrogen storage and transportation [4]. Therefore, the accurate prediction of hydrogen embrittlement is still a challenging topic.

Numerous efforts have been devoted to developing hydrogen-assisted fracture models driven by a variety of existing HE mechanisms. One of the most verified HE mechanisms is the hydrogen-enhanced localized plasticity (HELP) [5]. This mechanism states that hydrogen atoms lower the resistance of dislocation motion, and the enhanced localized plastic flow triggers earlier local cracking. Based on the concept of HELP, HE prediction models were developed [6–8]. For example, applying softened local flow stress suggested by Sofronis et al. [9], Liang et al. [10] and Ahn et al. [11,12] developed a HELP-dominated cohesive zone model (CZM), where a HELP-informed representative volume element (RVE) containing a spherical void is employed to describe traction-separation law (TSL). An extension of the conventional microvoids-based Gurson–Tvergaard–Needleman model to HE was done by Yu et al. [13]. They introduced a model for hydrogen-facilitated micro-void growth & coalescence (MVC). Kim et al. [14], Huang et al. [15,16] and Youn et al. [17] integrated HELP mechanism into the multi-axial fracture strain model. These studies highlighted that hydrogen's influence on dislocation behavior or vacancy formation facilitates MVC. However, plasticity-based HE prediction is still debatable because hydrogen-enhanced plasticity does not always been observed as the dominating mechanism [18]. Besides, HELP mechanism is also considered much too weak to trigger significant ductility loss [19].

In many experiment cases, using the hydrogen-enhanced decohesion (HEDE) mechanism is preferable. HEDE mechanism states that hydrogen reduces the bonding strength between metal atoms. The simulation of HEDE mechanism has been developed with the help of the cohesive zone model (CZM). By defining hydrogen-dependent cohesive strength, it has been successfully used to reproduce many experimental results [20]. Recently, phase field fracture models were developed based on HEDE mechanism to simulate engineering scale HE problems, where arbitrary cracking path simulation is allowed [21–24]. Nevertheless, some evidence indicated that HEDE solely could not rationalize the high sensitivity of embrittle under very low hydrogen concentrations [25].

Although HEDE or plasticity-based mechanism works well under some verified conditions, there is a growing consensus that the coexistence of multiple mechanisms governs the hydrogen embrittlement phenomenon [18,26–28]. Djukic et al. [26] has discussed the synergistic action of HELP and HEDE mechanism. As reviewed, HELP or HEDE could operate independently, cooperatively, or competitively. The specific hydrogen damage behavior depends strongly on the local situation (microstructure, hydrogen concentration, local stress). Recently, microstructural characterization has revealed enhanced dislocation activity beneath the hydrogen-induced cleavage surface, which implies that the critical hydrogen concentration responsible for local cleavage is strongly related to the dislocation activity. Novak et al. [29] and Nagao et al. [30] developed models for HE in high-strength martensitic steel, emphasizing HELP-induced local hydrogen accumulation enhancing HEDE. Similarly, Falkenberg et al. [31] and Brocks et al. [32] considered HELP-facilitated HEDE through a CZM-based method. These works demonstrated how HELP and HEDE work cooperatively. On the other hand, the competition effect among potential embrittlement mechanisms is also critical. Recently, Lin et al. [33,34] has developed a predictive model unifying hydrogen-enhanced plasticity and decohesion. Their model considered a complete Gurson model to account for HELP-promoted void evolution and HEDE-reduced local critical stress, which captured the competition between MVC and decohesion, but the cooperation effect, such as HELP-mediated HEDE, was not included. Liang et al. [35] investigated brittle cleavage and ductile fracture competition with Molecular Dynamics (MD) and Density functional theory (DFT) simulations. The results indicated that the dominant hydrogen embrittlement mechanism depends on the specific grain boundary type when multiple HE mechanisms coexist and interact with each other. The output of HE varies according to situations, which cannot be enveloped by any single mechanism.

According to the abovementioned state of the art, a gap exists in understanding the interplay among multiple HE mechanisms and their influence on HE phenomenon. To our best knowledge, at least three problems should be addressed:

(1) Fracture mode transition dominated by competition plasticity-based (HELP) and HEDE mechanism.
(2) Fracture criterion controlled by cooperation among multiple embrittlement mechanisms.
(3) Embrittlement kinetics based on local hydrogen diffusion and trapping, which connects hydrogen concentration with the deformation of a solid.

In this work, we tried to develop a HE prediction model accounting for the interaction between two popular hydrogen embrittlement mechanisms. i.e., HELP and HEDE. To this end, an independent ductile & brittle fracture model and the interacting law between them were proposed. Numerical simulation of the tensile test and fracture toughness test were conducted to show the performance. This work provides a powerful tool for a more realistic description of HE phenomenon.

Theoretical model for hydrogen embrittlement

Hydrogen concentration model

The model proposed by Sofronis et al. [9] is used to calculate hydrogen concentration, where hydrogen is assumed to reside at normal interstitial lattice sites (NILS) and hydrogen traps. NILS hydrogen concentration in stressed state is stated as

$$\frac{\theta_L}{1-\theta_L}=\frac{\theta_L^0}{1-\theta_L^0}K_L \tag{1}$$

where θ_L and θ_L^0 are the NILS hydrogen occupancy in stressed and unstressed state. Equilibrium coefficient K_L is

$$K_L=\exp\left(\frac{\sigma_m V_H}{RT}\right) \tag{2}$$

where $\sigma_m = 1/3\sigma_{ii}$ is the mean stress. V_H is the partial molar volume of hydrogen. R and T are the ideal gas constant and temperature in Kelvin. According to Oriani's theory [36,37], hydrogen concentration in trap is given as

$$\frac{\theta_T^{(i)}}{1-\theta_T^{(i)}}=\frac{\theta_L}{1-\theta_L}K_T^{(i)} \tag{3}$$

where $\theta_T^{(i)}$ represents the hydrogen occupancy in the i-th type hydrogen trap. $K_T^{(i)}$ is the equilibrium coefficient of i-th type trap,

$$K_T^{(i)}=\exp\left(\frac{W_B^{(i)}}{RT}\right) \tag{4}$$

where $W_B^{(i)}$ is the binding energy of i-th kind of hydrogen trap. Accordingly, hydrogen concentration can be expressed as (measured in H atom/metal atom)

$$\begin{aligned} c_L &= \beta\theta_L \\ c_T^{(i)} &= \theta_T^{(i)}\frac{N_T^{(i)}}{N_L} \end{aligned} \tag{5}$$

where β is the number of hydrogen bonding sites per metal atom. $\beta = 6$ is chosen for body-centered cubic (bcc) lattice [38]. N_L is the number of metal atom per volume. $N_T^{(i)}$ is the density of the i-th type hydrogen trap (measured in sites/m^3).

Damage models of HELP and HEDE mechanisms

Ductile tearing accounting for HELP mechanism

HELP mechanism states that hydrogen around dislocations will increase the mobility of dislocations [5]. One consequence of this change in dislocation behavior is the acceleration of local plastic flow, which promotes the evolution of MVC. The idea of HELP-enhanced MVC served as the theoretical foundation for many HE models on continuum scale. For example, the hydrogen-informed Gurson model developed by Yu et al. [13] and hydrogen-modified fracture strain model suggested by Kim et al. [14] and Huang et al. [16]. In the present work, we proposed a simplified form of hydrogen-modified fracture strain to evaluate the effect of HELP.

According to the model of Sofronis et al. [19,39], the impact of HELP mechanism on local plastic behavior can be manifested by a local flow stress

$$\sigma_f = \sigma_0\varphi(c) \tag{6}$$

where σ_0 is the local flow stress without hydrogen. The suggested expression of φ is

$$\varphi(c)=1-\xi\frac{c_{HELP}}{c_L^0} \tag{7}$$

where ξ is a model parameter describing the intensity of HELP's influence. c_{HELP} is the contributing hydrogen concentration. C_L^0 is a reference value of hydrogen concentration. According to atomic simulation [40–42], hydrogen atoms around dislocations can affect dislocation mobility. Therefore, c_{HELP} is assumed to be the summation of NILS hydrogen c_L and dislocation trapped hydrogen $C_T^{(d)}$

$$c_{HELP}=c_L+c_T^{(d)} \tag{8}$$

By assuming power-law hardening behavior of material, the relationship between original and HELP-informed flow criterion can be stated as

$$\sigma_0\left(1+\frac{\varepsilon_p}{\varepsilon_0}\right)^n=\sigma_f\left(1+\frac{\varepsilon_{pc}}{\varepsilon_0}\right)^n \tag{9}$$

where ε_p and ε_{pc} are the equivalent plastic strain with and without HELP's influence. ε_0 is the maximal elastic strain. n is the exponent of strain hardening. This relationship ignored the influence of yield surface shifting on local stress state, which is a simplified estimation of local stress redistribution induced by hydrogen. Accordingly, the HELP-enhanced equivalent plastic strain is governed by following nonlinear equation set implicitly

$$\begin{cases} \varepsilon_{pc}=\left(1-\xi\dfrac{c_{HELP}}{c_L^0}\right)^{-n}(\varepsilon_0+\varepsilon_p)-\varepsilon_0 \\ c_{HELP}=c_L+c_T^d(\varepsilon_{pc}) \end{cases} \tag{10}$$

According to Huang et al. [16], multi-axial fracture strain can be described as a function of local stress triaxiality and hydrogen concentration, the expression of fracture strain is given as

$$\varepsilon_f(c)=A\exp\left(B\frac{\sigma_m}{\sigma_{mises}\varphi(c)}\right)+C \tag{11}$$

where A, B and C are the model parameters [43], σ_m the mean stress and σ_{mises} is the Mises equivalent stress. Ductile fracture is assumed to occur when accumulated ductile damage over a loading history t reaches critical value. The accumulated damage ω_d is calculated with

$$\omega_d=\int_0^t\frac{\varepsilon_{pc}}{\varepsilon_f}\mathrm{d}t \tag{12}$$

where ε^p is the equivalent plastic strain. The failure criterion of ductile fracture is

$$\omega_d=\omega_c \tag{13}$$

where ω_c is the critical ductile damage.

Cleavage fracture accounting for HEDE mechanism

Cleavage is the most representative fracture mode in hydrogen environment. The brittle fracture induced by HEDE mechanism can be described by classical Griffith fracture theory. Under the assumption of plane strain state, the critical stress corresponding to an existing micro-crack with a length of $2a$ is stated as

$$\sigma_c = \sqrt{\frac{EG_{IH}}{\pi(1-\nu^2)a}} \tag{14}$$

where G_{IH} is the critical surface energy release rate accounting for hydrogen influence, a is the half-length of crack. E is Young's modulus and ν is Poisson's ratio. HEDE mechanism states that hydrogen atoms reduce the energy required to separate atomic planes. According to atomic calculations [44,45], the degradation induced by HEDE mechanism can be described as

$$G_{IH}(c) = \varphi(c)G_{Ic} = (1-\chi\theta)G_{Ic} \tag{15}$$

where G_{Ic} is the critical surface energy release rate without hydrogen's influence, χ is the model factor describing the intensity of HEDE. The hydrogen coverage θ, defined as the ratio between hydrogen concentration and saturated hydrogen concentration on the crack plane, is the driving force of degradation. For the intergranular (IG) or transgranular (TG) cleavage origins at boundary (denoted by $i = b$), θ is calculated as

$$\theta = \frac{\theta_T^{(b)} N_T^{(b)}}{N_T^{(b)}} = \theta_T^{(b)} \tag{16}$$

Noteworthy, due to the restriction of the continuum mechanics framework, the specific crack propagation path which eventually results in IG or TG cannot be distinguished. However, we assumed a critical event that cracks initiate at grain boundaries where trap binding energy is higher than dislocations. This assumption usually matches the situation of hydrogen-assisted fracture.

Cleavage fracture is usually predicted with the Beremin model. Generally, calculating fracture driving force requires the integration of maximal principal stress within the fracture control zone, which cannot be applied when calculating hydrogen damage. To overcome this problem, Kim et al. [46] had proven that maximal principal stress within an element can be used as a local cleavage fracture criterion. Accordingly, the maximal principal stress criterion for cleavage fracture is stated as

$$\sigma_1 = \sigma_c \tag{17}$$

HELP & HEDE interaction model

The competition behavior between HELP and HEDE has been verified by experiment observation [18,26,47]. For instance, Dong et al. [48] discovered that the interaction between hydrogen-induced plasticity and decohesion controls the cracking path inside ferrite grains in a hydrogen-charged dual-phase high-strength steel. The crack first propagates straightly along {100} planes. Afterward, the path deviates from the cleavage planes, indicating a fracture mechanism change from HEDE to hydrogen-enhanced plasticity, most probability HELP. According to Djukic et al. [49], the fracture surface of a hydrogen-charged carbon steel exhibited a mixture of micro-void coalescence, quasi-cleavage, and intergranular cracking, suggesting various active HE processes (mainly HEDE and HELP) affect local fracture events simultaneously. Meanwhile, atomic computations and material characterizations supported the cooperation between HELP and HEDE, also known as HELP-mediated HEDE. Martin et al. [50], Nagao et al. [51], and Wang et al. [52] discovered enhanced dislocation mobility beneath the intergranular fracture surface in hydrogen-embrittled iron and ferritic steel. Atomic simulation provided evidence of dislocation activity in hydrogen-affected grain boundary decohesion [25]. Above findings show that depending on the local hydrogen and stress conditions, HELP and HEDE-dominated failure can be competitive. In order to assess the competition effect, we applied the ductile-brittle transition model of Kim et al. [46]. The suggested failure criterion is

$$D = \max\left(\frac{\omega_d}{\omega_c}, \frac{\sigma_1}{\sigma_c}\right) \tag{18}$$

where D denotes damage state of material and $D = 1$ implies occur of failure.

HELP-mediated HEDE is assumed to be the primary cooperative behavior between HELP and HEDE. We considered the local crack process origins at the grain boundary described in Fig. 1(a). During local plastic deformation, hydrogen is transported by both lattice diffusion and dislocation slips. According to Oriani's trap theory [36,37], the local hydrogen population is controlled by the equilibrium between hydrogen occupancy in trap sites and NILS, as is shown in Fig. 1(b). When dislocation piles up against the grain boundary, dislocation hydrogen transportation provides additional hydrogen atoms in addition to the original boundary-lattice hydrogen equilibrate state. Since the binding energy of the boundary trap is usually higher than the dislocation trap, the newly developed equilibrate state tends to enhance the hydrogen population in boundary traps, which is an energy-favorable process. Such dislocation hydrogen transportation acts as an additional hydrogen source for local decohesion, as is exhibited in Fig. 1(c). When dislocation annihilation at the boundary, the hydrogen stored in dislocations is released into the NILS nearby, this can also produce a higher local lattice hydrogen concentration near the boundary trap sites, as shown in Fig. 1(d). Consequentially, a locally high hydrogen concentration c_L^{loc} is possible near the boundary, which can be expressed as

$$c_L^{loc} = c_L + \mu c_T^{(d)} \tag{19}$$

where c_L is the NILS hydrogen concentration, $c_T^{(d)}$ is the dislocation trapped hydrogen concentration. Parameter μ denotes the percentage of hydrogen atoms that participate HEDE. Accordingly, hydrogen coverage $\theta_T^{(bd)}$ after HELP-enhanced decohesion is stated as

$$\frac{\theta_T^{(bd)}}{1-\theta_T^{(bd)}} = \frac{\theta_L'}{1-\theta_L'} K_T^{(b)} \tag{20}$$

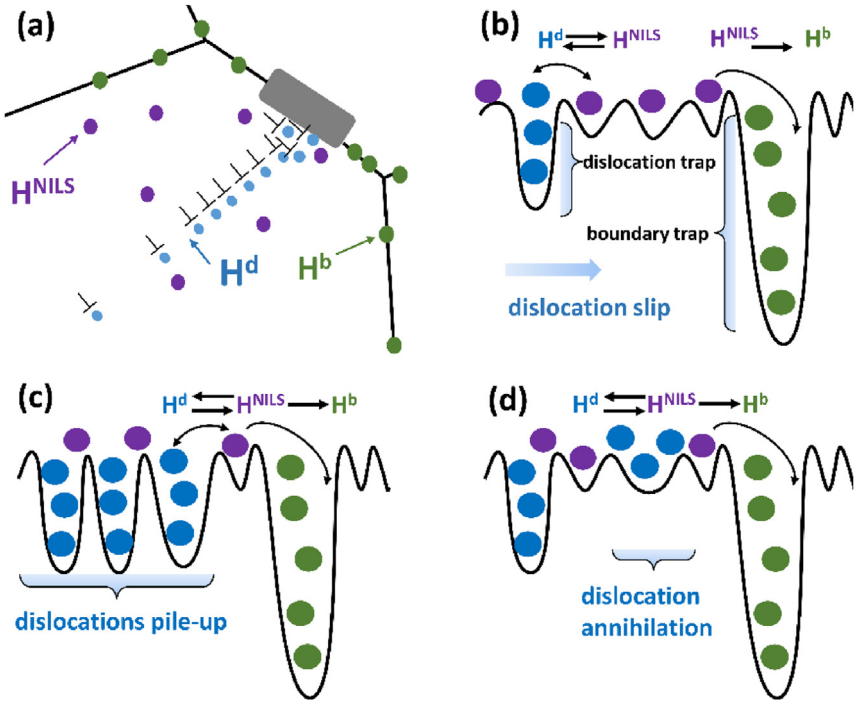

Fig. 1 – Illustration of HELP enhanced HEDE model: (a) local cracking model; (b) energy states of hydrogen atoms in traps; (c) energy states of hydrogen atoms at dislocation pile-up against boundary; (d) energy states of hydrogen atoms at dislocation annihilation at boundary.

where θ_L' is the hydrogen occupancy of NILS after HELP-enhanced decohesion

$$\theta'_L = \frac{c_L^{loc}}{\beta} = \theta_L + \mu \frac{1}{\beta} \theta_T^{(d)} \frac{N_T^{(d)}}{N_L} \tag{21}$$

The second term in the right hand of Equation (21) becomes negligible when dislocation-enhanced decohesion is not dominating, i.e., $\mu << 1$ or $N_T^{(d)} << N_L$. This situation corresponds to the cases where the dislocation-boundary hydrogen transmission is weak or high local hydrogen concentration induces cleavage before plastic flow occurs.

The proposed method for HELP & HEDE interplay is summarized in Fig. 2. The method contains a ductile-brittle damage model driven by local hydrogen concentration around the specific type of hydrogen traps. The competition effect is governed by the failure criterion in Equation (18). The cooperation effect is described by dislocation-enhanced hydrogen accumulation shown in Equation (19)~Equation (21). It is important to note that the models presented should not be restricted as only options for ductile and brittle damage evaluation. Other models based on single HELP or HEDE mechanism can be used to evaluate the potential of hydrogen-induced ductile and brittle fracture. For example, the H-informed Gurson model [13] and the HELP-driven CZM model proposed by Ahn et al. [11] are candidates for hydrogen-enhanced plasticity. On the other hand, phase field method [53] or CZM [54] models can be used to describe HEDE mechanism. However, it is emphasized that the HELP mechanism should be driven by the sum of local hydrogen concentration in lattice and dislocation traps. The decohesion should be induced by hydrogen trapped on the potential cracking plane.

Model verification and application

Numerical implementation

The proposed method was implemented on the Commercial Software package ABAQUS with user subroutine VUSDFLD. In an increment, the stress-strain data at an integration point was passed into VUSDFLD subroutine. Then, hydrogen concentration and enhanced localized plastic strain induced by HELP mechanism were calculated. The output was used to calculate accumulated ductile and brittle damage with hydrogen-informed damage evolution laws. Finally, the damages were evaluated for failure. Element deletion was conducted for the failure element, and the stiffness of the model degraded. In order to overcome the numerical stability problem raised by crack propagation, explicit dynamic analysis was used with a guaranteed quasi-static state (the ratio between internal energy and kinetic energy of the system keeps larger than 1000).

Example 1: hydrogen-charged SSRT test

Material properties

We considered an assumed material to exhibit the performance of the proposed method. This material was assumed to obey the power-law hardening rule with exponent $n = 0.1$ and initial yield stress $\sigma_0 = 400$ MPa. Table 1 lists the parameters of the assumed material.

SSRT simulation under different hydrogen concentration

The investigated specimen is a smooth round bar with a diameter of 6 mm and a gauge of 25 mm. Fig. 3 illustrates the

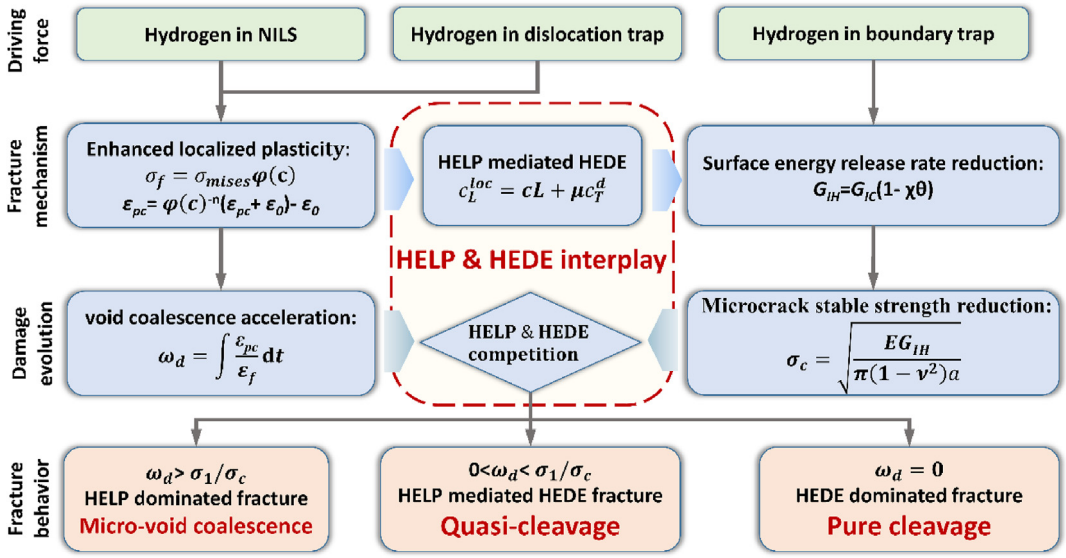

Fig. 2 – Unifying HELP + HEDE model.

configuration and finite element model. The problem was considered a 2D axisymmetric problem. A 1/2 axisymmetric finite element model was established for the gauged part of the specimen. The mesh in the middle part (failure zone) was refined to 0.1mm × 0.1 mm.

Table 1 – Model parameters of assumed material.

Parameter	Value	Reference
Partial molar volume of Hydrogen, V_H	2.0×10^{-6} m^3/mol	[9]
Molar volume of metal, V_M	7.11×10^{-6} m^3/mol	
Hydrogen bonding sites in NILS, β	6	[38]
Binding energy of dislocation trap, $W_B^{(d)}$	20.0 kJ/mol	assumed
Binding energy of grain boundary, $W_B^{(gb)}$	40.0 kJ/mol	
Parameter of dislocation induced decohesion, μ	0.2	
Density of grain boundary trap, $N_T^{(gb)}$	5.0×10^{23} sites/m^3	
Density of dislocation trap, $N_T^{(d)}$	$10^{27.23-2.33\exp(-5.5\varepsilon p)}$ sites/m^3	[44]
Model parameter of multi-axial fracture strain model, A	3.5	assumed
Model parameter of multi-axial fracture strain model, B	−1.5	
Model parameter of multi-axial fracture strain model, C	0.0	
Surface energy release rate, G_{Ic}	60 kJ/mol	
Critical crack size, a	0.0005 mm	
Damage parameter of HELP, ξ	0.01	
Damage parameter of HEDE, χ	0.89	[45]

The simulations were conducted under different hydrogen concentrations. Hydrogen concentration in un-stressed state was set as 0.0wppm (air), 0.003 wppm, 0.1 wppm, and 1.0wppm. Then the specimens were loaded at both ends with a constant velocity until rupture.

Simulation results

Fig. 4(a) displays the simulated engineering stress-strain curves, and the profile of ruptured specimens is exhibited in Fig. 4(b). The results indicate that both elongation and

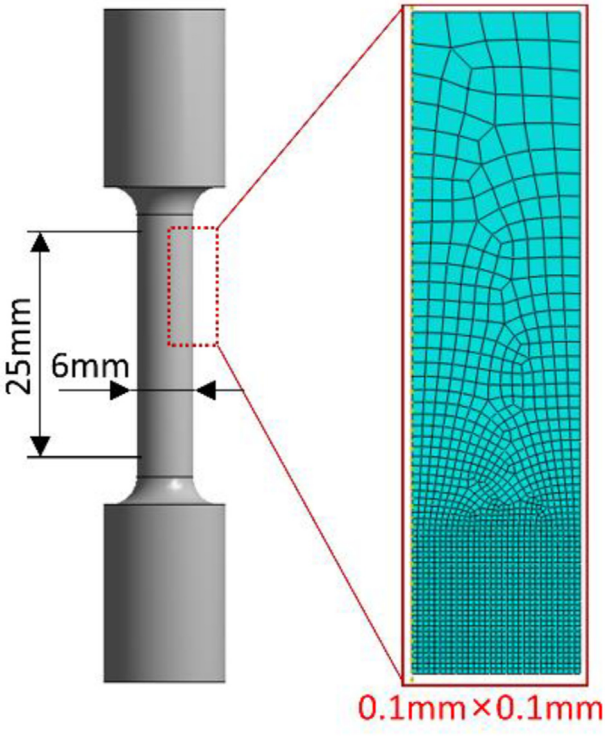

Fig. 3 – Configuration and mesh of SSRT specimen.

reduction of area reduced as hydrogen concentration increases. Given that these properties are usually considered indexes of plasticity, the results imply the prediction of different HE levels.

Assigning elongation as the index, Fig. 5 illustrates the predicted trends, highlighting the competition and cooperation between the HELP & HEDE mechanism. It is shown that all curves, whether driven by HELP, HEDE, or coupled mechanism (HELP + HEDE), decrease with increasing hydrogen concentration. However, single HELP provokes only little ductility loss even in a high hydrogen concentration environment, as is shown by the yellow line, which matches the conclusion of Liang et al. [35]. HEDE leads to a significant reduction of elongation, but rupture is difficult at a low hydrogen concentration, according to the red line. As the blue line indicates, HELP + HEDE prediction leads to a transition from HELP to HEDE mechanism at about 0.03 wppm hydrogen concentration. Thus, the competition between the two mechanisms yields a threshold effect for influential hydrogen embrittlement. Below the threshold, HELP mechanism controls hydrogen damage, and the influence on the mechanical property is weak. When hydrogen concentration elevates, the impact of HE becomes more significant as HEDE mechanism becomes dominated.

Fig. 6 illustrates the parametric study result on parameters governing HELP, HEDE, and their interaction. Fig. 6(a) exhibits the impact of ξ on fracture in HELP only case. It is clear that a higher value of ξ, indicating more localized softening as a consequence of HELP, which leads to more reduction of ductility. However, no severe HELP-induced damage was observed even in high hydrogen concentration cases. Fig. 6(b), which studies HEDE effect, demonstrates that the increase of parameter χ produced increasingly pronounced degradation. Unlike the trends in the HELP-only case, the HEDE mechanism induced sharp degradation of the ductility within a narrow hydrogen concentration range. The HEDE-induced damage trends to be saturated under very high hydrogen concentration, but it also produced unreasonably high ductility in low hydrogen concentration cases, which means it is unsuitable for low hydrogen concentration cases. Fig. 6(c) plots the influence of parameter μ on HELP mediated HEDE effect. Accordingly, a higher value of μ leads to a more significant cooperation effect, which produces lower elongation at the same hydrogen concentration. The underlying is that the more dislocation-transported hydrogen atoms contribute weakening of cohesive strength, the easier decohesion will be.

Fig. 7 illustrates the evolution of the ratio between boundary trap hydrogen coverage with and without HELP effect, $\theta_T^{(bd)}/\theta_T^{(b)}$ ($\mu = 0.6$). The results indicate the intensity of HELP mediated HEDE effect. A value more significant than 1.0 implies that HELP promotes hydrogen coverage. Accordingly, the effect of HELP-mediated HEDE is enhanced as strain increases. Besides, the effect is more pronounced in the lower hydrogen concentration case. When hydrogen concentration becomes larger than 0.5 wppm, the effect of HELP-mediated HEDE almost disappears as the hydrogen coverage is nearly saturated.

Discussions

According to the results shown in Fig. 5–7, the proposed HE prediction method reproduces some mechanical behavior in hydrogen environment. With respect to mechanical properties degradation, the proposed model implies more serious hydrogen embrittlement when hydrogen concentration elevates. From existing SSRT experiments in hydrogen environments, hydrogen-induced reduction of elongation (EL) and reduction of area (RA) were reported. For example, Meng et al. [55] performed SSRT experiments in 12 MPa N2/H2 mixture gas. According to which, elongation reduced from 26.9% to

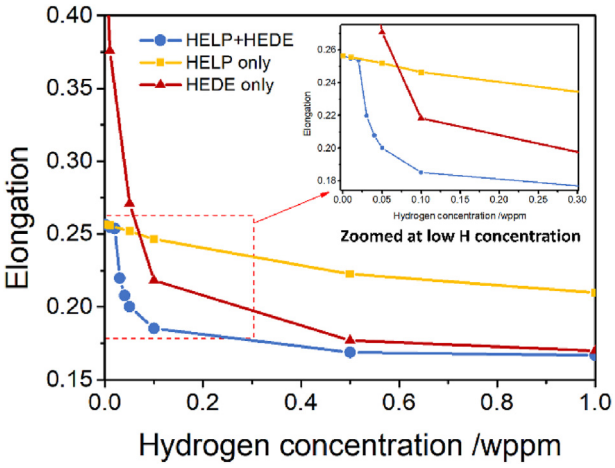

Fig. 5 – HELP & HEDE interplay in tensile simulation.

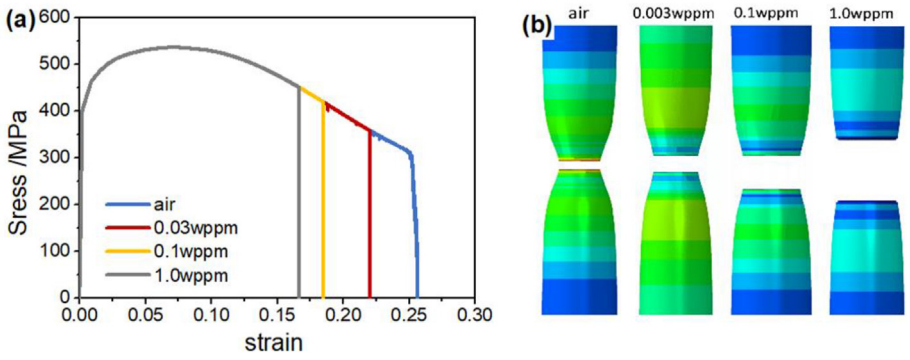

Fig. 4 – Tensile simulation in hydrogen environment: (a) reduced elongation; (b) reduced reduction of area.

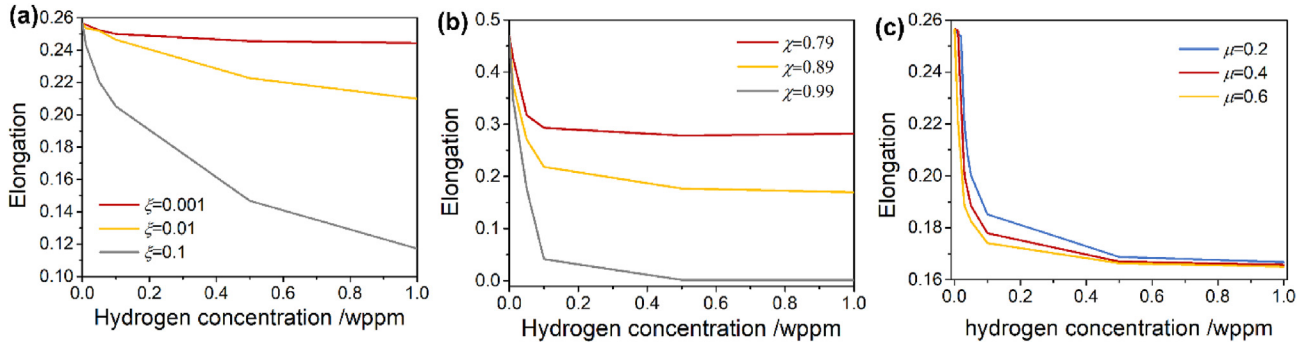

Fig. 6 – Parametric study of damage parameters: (a) HELP only; (b) HEDE only; (c) HELP mediated HEDE.

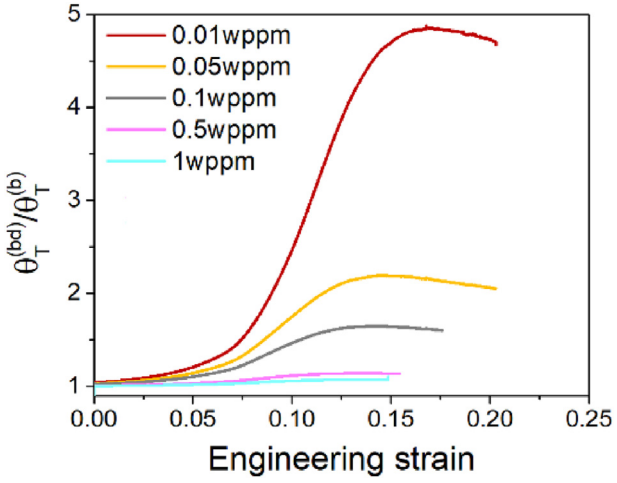

Fig. 7 – Evolution of HELP mediated HEDE effect under different hydrogen concentration.

21.9% as the hydrogen volume fraction rose from 0 to 50%. Nguyen et al. [56] performed SSRT of SA372 steel in 10 MPa and 99 MPa hydrogen environments. The reported elongation was 11.3% in 10 MPa H_2 and 8.8% in 99 MPa H_2, which is significantly reduced from the value of 20.1% in air. Their results showed that the difference between air and 10 MPa H_2 is more significant than between 10 MPa and 99 MPa H_2. These facts coincide with the predicted feature of the proposed model.

Regarding the damage mechanism prediction, HELP mechanism was activated under low hydrogen concentration cases. As hydrogen concentration increases, the dominant mechanism shift from HELP to HELP-mediated HEDE. Finally, HEDE mechanism will dominate the fracture process. Hüter et al. [57] analyzed fracture of hydrogen-charged martensitic steel. Accordingly, under low hydrogen concentration (1.5 ppm), the fracture surface is featured by shallow dimples, indicating HELP mechanism activated at this condition. Under 5 ppm hydrogen charged, the fracture is characterized by a mixture of micro-voids, TG, and IG cleavage. Further increasing of hydrogen concentration led to more prominent TG and IG features. These findings imply the shift of dominating mechanism from HELP to HEDE. Dujkic et al. [26] has systematically reviewed the effect of hydrogen in various steels. They concluded a unified model for the synergistic interplay of HE mechanisms in steel based on the experiment observations over decades, where HELP and HEDE mechanism cooperates in a manner of HELP to HEDE transition as hydrogen concentration increases. This evidence supports the rationality of the proposed HELP & HEDE competition model.

According to Fig. 7, HELP-mediated HEDE effect tends to be suppressed with increasing hydrogen concentration. HELP mechanism plays an important role even in fully brittle hydrogen-assisted fracture cases. As emphasized by Martin et al. [5], dislocation-mediated decohesion mechanism whereby hydrogen-influenced dislocation promotes hydrogen accumulation is a possible mechanism to compensate for the insufficiency of HEDE mechanism in reducing strength. However, the predominant activity of HELP mechanism was only sometimes necessary. Some studies observed hydrogen-induced dislocation pin-up instead of dislocation motion [58,59]. The suppression of dislocation-mediated decohesion is attributed to high hydrogen concentration at interfaces which is sufficient to trigger decohesion. The hydrogen concentration in hydrogen traps is positively related to hydrogen concentration. Therefore, higher environment hydrogen concentration is expected to lead to less HELP-mediated HEDE, as is reproduced by the proposed method.

Example 2: prediction on hydrogen environment fracture of 4130 steel

In engineering practice, fracture toughness in hydrogen environment and hydrogen-assisted cracking (HIC) threshold stress intensity factor were used to evaluate the fracture resistance in hydrogen environment. However, a significant difference exists between the two test methods' hydrogen damage kinetics. In the fracture toughness test, deformation, hydrogen diffusion co-occur, and local plastic flow contribute to the fracture process, which leads to interaction between dislocation-based and interface-based hydrogen damage. In hydrogen-assisted cracking threshold stress intensity factor test, the load was applied before the specimen was immersed into hydrogen environment, such hydrogen damage is mainly dominated by hydrogen-interface interplay. This difference usually results in an almost one-fold lower fracture toughness value than HIC threshold stress intensity factor in the same hydrogen environment [60], which is evidence of the coexistence of multiple hydrogen mechanisms. For further illustration, fracture toughness and threshold stress intensity factor

Table 2 – Material properties of 4130X steel reported in Ref. [61].

Material property/parameter	Yield stress	Tensile stress	Elongation	Parameter K	Parameter n
Value	700 MPa	830 MPa	18.2%	1110	0.075

Table 3 – Model parameters of AISI-4130 steel.

Parameter	Value	Reference
Partial molar volume of Hydrogen, V_H	2.0×10^{-6} m^3/mol	[9]
Molar volume of metal, V_M	7.11×10^{-6} m^3/mol	
Hydrogen bonding sites in NILS, β	6	[38]
Binding energy of dislocation trap, $W_B^{(d)}$	26.0 kJ/mol	[30]
Binding energy of grain boundary, $W_B^{(gb)}$	47.4 kJ/mol	
Density of grain boundary trap, $N_T^{(gb)}$	5.0×10^{23} sites/m^3	
Density of dislocation trap, $N_T^{(d)}$	$10^{27.23\text{-}2.33\exp(-5.5\varepsilon p)}$ sites/m^3	[44]
Model parameter of multi-axial fracture strain model, A	3.4	[61]
Model parameter of multi-axial fracture strain model, B	−1.5	
Model parameter of multi-axial fracture strain model, C	0	
Surface energy release rate, G_{Ic}	244 kJ/mol	[65]
Parameter of dislocation induced decohesion, μ	0.1	assumed
Critical crack size, a	0.0006 mm	assumed
Damage parameter of HELP, ξ	0.0005	assumed
Damage parameter of HEDE, χ	0.89	[45]

in hydrogen environment of high-strength steel AISI-4130 were predicted.

Model parameters

Constitutive relationship. The true stress-strain curve of 4130 steel used in the predictions was extracted from reference [61]. The constitutive relationship was assumed to obey a power exponent hardening law as is described in Equation (22). The reported data of 4130X steel is listed in Table 2.

$$\sigma_{ture} = K{\varepsilon_p}^n \tag{22}$$

Hydrogen concentration & trap properties. In hydrogen environment, the balance between hydrogen concentration in material and in environment is governed by Sievert's law. For 4130 steel, the available value was measured as [30].

$$C_L^0 = 108 \exp\left(\frac{-27200}{RT}\right)\sqrt{f}\ \text{mol H}_2\cdot\text{m}^{-3} \tag{23}$$

where f is the fugacity of gas measure in Pa. C_L^0 is hydrogen concentration in metal lattice in un-stress state. The dependency of fugacity on hydrogen pressure is

$$f = p \exp\left(\frac{pb}{RT}\right) \tag{24}$$

With $b = 15.84$ cm^3/mol.

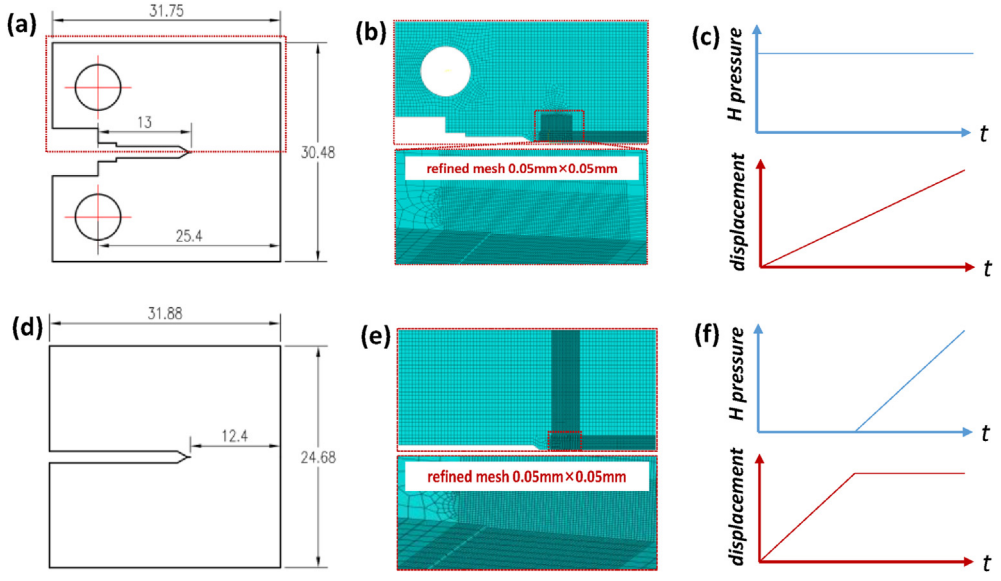

Fig. 8 – Illustration of fracture resistance simulation: (a) specimen for RDT; (b) mesh for RDT; (c) load condition for RDT; (d) specimen for CDT; (e) mesh for CDT; (f) load condition for CDT.

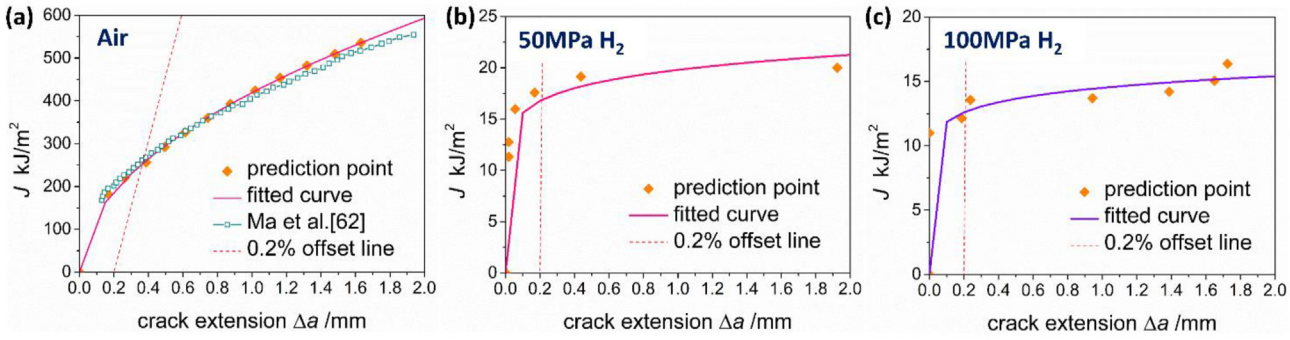

Fig. 9 – J–R curves prediction in different environment: (a) air; (b) 50 MPa H_2; (c) 100 MPa H_2.

For tempered martensitic steel, the binding energy of dislocation has been measured and calculated [29,30]. The value varies in a range of 18~36 kJ/mol. In this work, dislocation trap binding energy was chosen as $W_B^{(d)} = 26.0$ kJ/mol, which is in accordance with the work of Nagao et al. [30]. Referring to the works on AISI 4140 performed by Zafra et al. [62] and Colombo et al. [44], the trap density of dislocation was assumed as

$$N_T^{(d)} = 10^{27.23-2.33\exp(-5.5\varepsilon_p)} \quad (25)$$

The binding energy and density of GB of martensitic steel have a strong dependency on the specific chemical composition and heat treatment condition. Here, the values of Nagao et al. [30] was adopted. The binding energy and trap density of GB were $W_B^{(d)} = 47.4$ kJ/mol and $N_T^{(gb)} = 5.0 \times 10^{23}$ sites/m^3 respectively.

Hydrogen damage model parameters. Based on the experiment of Ma et al. [61] for 4130X steel. The parameters for fracture strain calculation were determined as $A = 3.4$, $B = -1.5$, and $C = 0$. The HELP coefficient was set as $\xi = 0.001$. This value is determined based on the assumption that hydrogen's effect on the flow stress is about 5% in 100 MPa H_2, which follows the trend observed from the hydrogen-charged tensile test of this material [61,63,64].

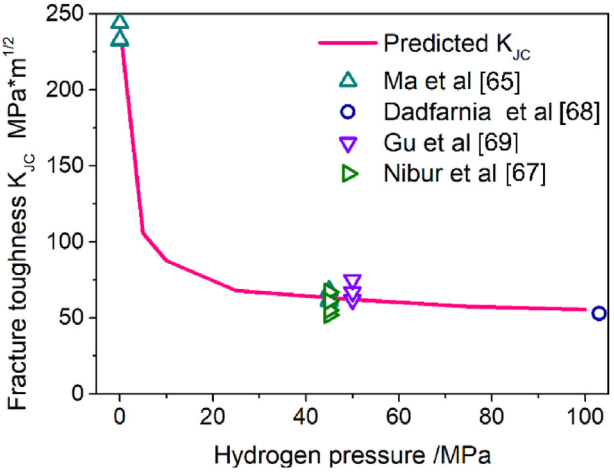

Fig. 10 – Fracture toughness prediction results.

The critical surface energy release rate G_{IC} was assumed to equal the elastoplastic fracture toughness of material J_{IC}. $G_{IC} = 244$ kJ/m^2 was chosen according to Ma et al. [65]. In the Griffith fracture model, the initial crack length can be obtained from the statistical analysis of metallographic photos. In this work, $a = 0.6$ μm was assumed for the best fitness of experiment results. For the interacting coefficient of HELP & HEDE, $\mu = 0.1$ was adopted in the present work. For the HEDE model, the value of coefficient χ was determined by linear regression of atomic calculation results [24,66], which yields $\chi = 0.89$.

All the determined parameters for AISI 4130 steel are listed in Table 3.

Prediction method

The rising displacement test (RDT) was simulated to predict the elastoplastic fracture toughness K_{JC} (converted from J_{IC}) following ASTM E1820. The constant displacement test (CDT) was simulated to predict HIC threshold stress intensity factor K_{THa} following ASTM E1681. The standard CT specimens with a thickness of 12.7 mm were considered for both investigations. Fig. 8 displays the geometry and mesh of the specimens.

In the rising displacement test simulation, the hydrogen pressure was applied as the initial condition. Then, a rising displacement was applied to the loading holes, as is illustrated in Fig. 8(c). After the crack propagated, the crack length and applied force were extracted from the result. The fracture toughness $J_{C,H}$ was calculated and then converted into K_{JC} as per the method in ASTM E1820.

The constant displacement test simulation was implemented in two steps. In the first step, the specimen was loaded to a fixed displacement at its front surface, which applied a

Table 4 – Stress intensity factor threshold prediction results.

Hydrogen pressure/MPa	K_{app}/MPa·m$^{1/2}$	K_{THa}/MPa·m$^{1/2}$	Refs.
100	104.8	95.0	This work
	94.4	89.6	
	83.9	81.1	
90	108.7	85.7	[73]
	109.3	92.7	
103	189.0	98.0	[68]

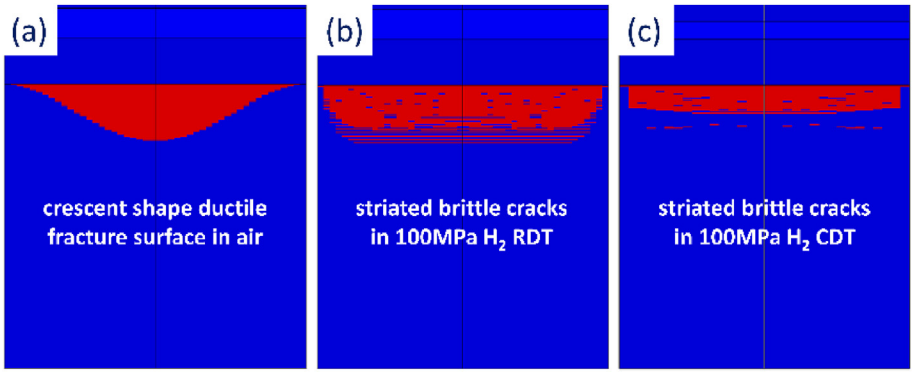

Fig. 11 – Cracking path predicted in different environment: (a) rising displacement test in air; (b) rising displacement test in 100 MPa H_2; (c) constant displacement test in 100 MPa H_2.

stress intensity factor at crack tip K_{app}. Hydrogen concentration was set as 0 in this step. In the second step, steptime-dependent hydrogen pressure was considered through VUSDFLD subroutine, as is illustrated in Fig. 8(f). As hydrogen concentration was assumed in equilibrate state. The second step calculates the hydrogen damage in different hydrogen pressure without the interference of displacement load. After the crack propagated, the crack length was extracted from the result. The stress intensity factor at crack arrested K_{THa} was calculated as per the method in ASTM E1681.

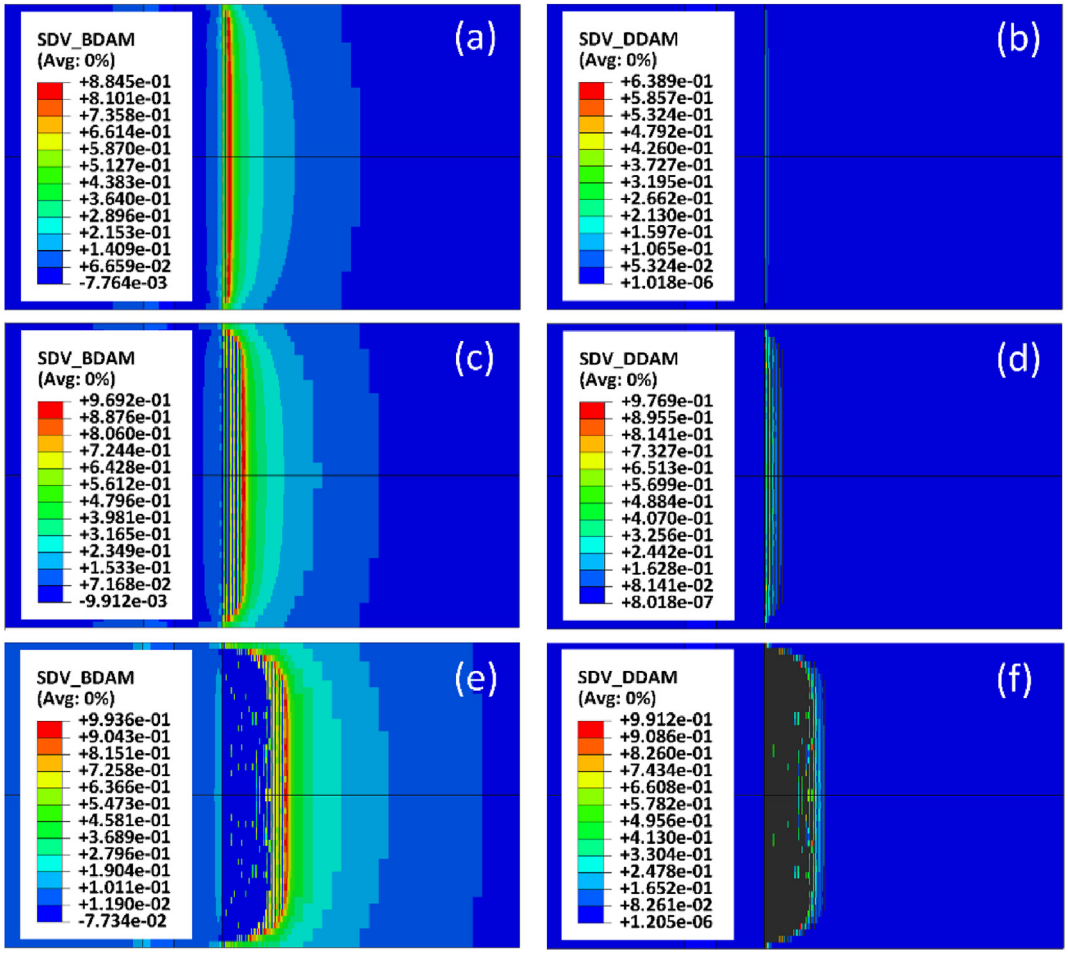

Fig. 12 – Damage evolution during crack propagation: (a) brittle damage at $U = 0.12$ mm; (b) ductile damage at $U = 0.12$ mm; (c) brittle damage at $U = 0.16$ mm; (d) ductile damage at $U = 0.16$ mm; (e) brittle damage at $U = 0.20$ mm; (f) ductile damage at $U = 0.20$ mm.

Prediction results and discussions

Fracture toughness. Fig. 9 plots the predicted J-R curves. Fig. 10 displays the predicted fracture toughness results. The fracture test data extracted from Ma et al. [65], Nibur et al. [67], Dadfarnia et al. [68], and Gu et al. [69] were selected for comparison. It is demonstrated that the fracture toughness reduced firstly quickly and then slowly as hydrogen pressure increased. The shape of the predicted curve in Fig. 10 coincides with the similar study results from Wang et al. [70], Olden et al. [71] and Thomas et al. [72]. At the typical service pressure condition of 4130 steel, the fracture toughness values predicted by the proposed method agree with the values in the literature. On the other hand, the results in Table .4 demonstrate the predicted stress intensity factor threshold K_{THa} at 100 MPa. The K_{THa} obtained by Dadfarnia et al. [68] at 103 MPa and Zhai et al. [73] at 90 MPa were selected for comparison. It can be found that the predicted result is in good agreement with the experimental results. In addition, it is demonstrated that predicted K_{THa} is higher than K_{JC} under the same hydrogen pressure. The higher value of HIC threshold stress intensity factor than fracture toughness has been experimentally observed [60,68]. This phenomenon was attributed to the difference in governing HE mechanism in the two test methods. Therefore, the results show that the proposed method can distinguish the difference in HE kinetic caused by the interaction between HELP and HEDE under different boundary conditions.

Fracture morphology. Fig. 11 shows the simulated crack propagation contour. It is shown in Fig. 11(a) that the crack contour generated in air shows a crescent shape, which is consistent with the typical fractographic feature of ductile fracture. In 100 MPa hydrogen environment, the crack contour exhibits brittle fracture characteristics featured by a flat crack front profile. In addition, Fig. 11(b) and (c) show striated brittle cracks beneath the crack tip. Fig. 12 shows the detailed evolution of ductile and brittle damage during crack propagation in 100 MPa H_2 (loading hole displacement denoted as U), Fig. 12(a) demonstrates that the brittle fracture criterion is met as the load increases, indicating brittle fracture governs the crack propagation. Meanwhile, a small amount of ductile damage accumulated was also activated, see Fig. 12(b). As the crack propagates, striated brittle cracks at intervals of about 100 μm (shown in Fig. 12(c)–12(e)) occurred beneath the crack tip. Significant plastic accumulation occurred in the remaining ligaments between the striations, which means the crack propagates in an alternating ductile (MVC) and brittle (QC or IG) way. In the literature [74], intermittent slow and fast growth region featured by MVC and IG was observed in martensitic high-strength steels fractured in hydrogen environment. The reproduction of this particular hydrogen-induced fracture fractographic feature supports the reasonability of the proposed method.

Conclusions

In this work, a hydrogen embrittlement prediction method was proposed for the coexistence of HELP and HEDE mechanisms. The law for the ductile & brittle fracture competition and the dislocation-enhanced decohesion were modeled. Following conclusions can be reached.

(1) The competition between HELP and HEDE was achieved by the synergistic evolution of a fracture strain-based ductile damage model and a stress-based brittle fracture model. The cooperation effect was captured by HELP-enhanced hydrogen coverage at boundary, which matches HELP-mediated HEDE concept.
(2) Hydrogen-dependent ductile to brittle transition was successfully simulated. Under low hydrogen concentration, hydrogen embrittlement is dominated by HELP mechanism. Under high hydrogen concentration, HEDE is the governing fracture mechanism, but HELP also contributes via HELP-mediated HEDE. As hydrogen concentration increases, HELP-mediated HEDE tends to be suppressed. All predicted features agree with existing experiment findings.
(3) In the investigated example, the proposed model reasonably predicted fracture toughness and HIC stress intensity factor threshold in hydrogen environment. The model automatically captures the difference in hydrogen damage kinetics inherent in the two test methods, which supports the rationality of the proposed strategy for HELP and HEDE interaction.

Declaration of competing interest

The authors declare that they have no known competing financial interests or personal relationships that could have appeared to influence the work reported in this paper.

Acknowledgement

This work was supported by the Jiangsu Province Engineering Research Center of High-Level Energy and Power Equipment(No.JSNYDL-202201). The financial support of SINOPEC was also acknowledged.

REFERENCES

[1] Martin ML, Connolly MJ, DelRio FW, Slifka AJ. Hydrogen embrittlement in ferritic steels. Appl Phys Rev 2020;7:41301.
[2] Hachet G, Li J, Hallil AM, Metsue A, Oudriss A, Bouhattate J, et al. A multi-scale analysis of the different interactions between defects and hydrogen: a review on the contribution of the elastic fields. Eng Fract Mech 2019;218:106621.
[3] Dwivedi SK, Vishwakarma M. Effect of hydrogen in advanced high strength steel materials. Int J Hydrogen Energy 2019;44:28007–30.
[4] Meda US, Bhat N, Pandey A, Subramanya KN, Lourdu Antony Raj MA. Challenges associated with hydrogen storage systems due to the hydrogen embrittlement of high strength steels. Int J Hydrogen Energy 2023;48:17894–913.

[5] Martin ML, Dadfarnia M, Nagao A, Wang S, Sofronis P. Enumeration of the hydrogen-enhanced localized plasticity mechanism for hydrogen embrittlement in structural materials. Acta Mater 2019;165:734–50.
[6] Gong P, Turk A, Nutter J, Yu F, Wynne B, Rivera-Diaz-del-Castillo P, et al. Hydrogen embrittlement mechanisms in advanced high strength steel. Acta Mater 2022;223:117488.
[7] Robertson IM, Sofronis P, Nagao A, Martin ML, Wang S, Gross DW, et al. Hydrogen embrittlement understood. Metall Mater Trans 2015;46:2323–41.
[8] Dadfarnia M, Nagao A, Wang S, Martin ML, Somerday BP, Sofronis P. Recent advances on hydrogen embrittlement of structural materials. Int J Fracture 2015;196:223–43.
[9] Sofronis P, Liang Y, Aravas N. Hydrogen induced shear localization of the plastic flow in metals and alloys. Eur J Mech Solid 2001;20:857–72.
[10] Liang Y, Ahn DC, Sofronis P, Dodds RH, Bammann D. Effect of hydrogen trapping on void growth and coalescence in metals and alloys. Mech Mater 2008;40:115–32.
[11] Ahn DC, Sofronis P, Dodds R. Modeling of hydrogen-assisted ductile crack propagation in metals and alloys. Int J Fracture 2007;145:135–57.
[12] Ahn DC, Sofronis P, Dodds RH. On hydrogen-induced plastic flow localization during void growth and coalescence. Int J Hydrogen Energy 2007;32:3734–42.
[13] Yu H, Olsen JS, Alvaro A, Qiao L, He J, Zhang Z. Hydrogen informed Gurson model for hydrogen embrittlement simulation. Eng Fract Mech 2019;217:106542.
[14] Kim N, Oh C, Kim Y, Yoon K, Ma Y. Hydrogen-assisted stress corrosion cracking simulation using the stress-modified fracture strain model. J Mech Sci Technol 2012;26:2631–8.
[15] Huang S, Hui H. Predictive environmental hydrogen embrittlement on fracture toughness of commercial ferritic steels with hydrogen-modified fracture strain model. Int J Hydrogen Energy 2022;47:10777–87.
[16] Huang S, Zhang Y, Yang C, Hu H. Fracture strain model for hydrogen embrittlement based on hydrogen enhanced localized plasticity mechanism. Int J Hydrogen Energy 2020;45:25541–54.
[17] Youn G, Kim Y, Kim J, Lam P. A fracture strain based numerical prediction method for hydrogen effect on fracture toughness. Int J Mech Sci 2021:202–3. 106492.
[18] Gerberich WW, Stauffer DD, Sofronis P. A coexistent view of hydrogen effects on mechanical behavior of crystals: HELP and HEDE. In: Somerday B SPJR, editor. International hydrogen Conference-effects of hydrogen on materials. ASM International, Jackons Lake Lodge, Grand Teton National Park, Wyoming, USA. Ohio; 2009. p. 38–45. 2008.
[19] Barrera O, Tarleton E, Tang HW, Cocks ACF. Modelling the coupling between hydrogen diffusion and the mechanical behaviour of metals. Comp Mater Sci 2016;122:219–28.
[20] Jemblie L, Olden V, Akselsen OM. A review of cohesive zone modelling as an approach for numerically assessing hydrogen embrittlement of steel structures. Philos Trans A Math Phys Eng Sci 2017;375.
[21] Isfandbod M, Martínez-Pañeda E. A mechanism-based multi-trap phase field model for hydrogen assisted fracture. Int J Plasticity 2021;144:103044.
[22] Kristensen PK, Niordson CF, Martínez-Pañeda E. Applications of phase field fracture in modelling hydrogen assisted failures. Theor Appl Fract Mech 2020;110:102837.
[23] Fernández-Sousa R, Betegón C, Martínez-Pañeda E. Analysis of the influence of microstructural traps on hydrogen assisted fatigue. Acta Mater 2020;199:253–63.
[24] Martínez-Pañeda E, Golahmar A, Niordson CF. A phase field formulation for hydrogen assisted cracking. Comput Method Appl M 2018;342:742–61.
[25] Wang S, Martin ML, Robertson IM, Sofronis P. Effect of hydrogen environment on the separation of Fe grain boundaries. Acta Mater 2016;107:279–88.
[26] Djukic MB, Bakic GM, Sijacki Zeravcic V, Sedmak A, Rajicic B. The synergistic action and interplay of hydrogen embrittlement mechanisms in steels and iron: localized plasticity and decohesion. Eng Fract Mech 2019;216:106528.
[27] Sun B, Krieger W, Rohwerder M, Ponge D, Raabe D. Dependence of hydrogen embrittlement mechanisms on microstructure-driven hydrogen distribution in medium Mn steels. Acta Mater 2020;183:313–28.
[28] Ding Y, Yu H, Lin M, Zhao K, Xiao S, Vinogradov A, et al. Hydrogen-enhanced grain boundary vacancy stockpiling causes transgranular to intergranular fracture transition. Acta Mater 2022;239:118279.
[29] Novak P, Yuan R, Somerday BP, Sofronis P, Ritchie RO. A statistical, physical-based, micro-mechanical model of hydrogen-induced intergranular fracture in steel. J Mech Phys Solids 2010;58:206–26.
[30] Nagao A, Dadfarnia M, Somerday BP, Sofronis P, Ritchie RO. Hydrogen-enhanced-plasticity mediated decohesion for hydrogen-induced intergranular and "quasi-cleavage" fracture of lath martensitic steels. J Mech Phys Solids 2018;112:403–30.
[31] Falkenberg R, Brocks W, Dietzel W, Scheider I. Modelling the effect of hydrogen on ductile tearing resistance of steels. Int J Mater Res 2010;101:989–96.
[32] Brocks W, Falkenberg R, Scheider I. Coupling aspects in the simulation of hydrogen-induced stress-corrosion cracking. Procedia IUTAM 2012;3:11–24.
[33] Lin M, Yu H, Ding Y, Wang G, Olden V, Alvaro A, et al. A predictive model unifying hydrogen enhanced plasticity and decohesion. Scripta Mater 2022;215:114707.
[34] Lin M, Yu H, Ding Y, Olden V, Alvaro A, He J, et al. Simulation of ductile-to-brittle transition combining complete Gurson model and CZM with application to hydrogen embrittlement. Eng Fract Mech 2022;268:108511.
[35] Liang S, Huang M, Zhao L, Zhu Y, Li Z. Effect of multiple hydrogen embrittlement mechanisms on crack propagation behavior of FCC metals: competition vs. synergy. Int J Plasticity 2021;143:103023.
[36] Oriani RA. The diffusion and trapping of hydrogen in steel. Acta Metall 1970;18:147–57.
[37] Oriani RA, Josephic PH. Equilibrium aspects of hydrogen-induced cracking of steels. Acta Metall 1974;22:1065–74.
[38] Krom AHM, Koers RWJ, Bakker A. Hydrogen transport near a blunting crack tip. J Mech Phys Solids 1999;47:971–92.
[39] Díaz A, Alegre JM, Cuesta II. Numerical simulation of hydrogen embrittlement and local triaxiality effects in notched specimens. Theor Appl Fract Mech 2017;90:294–302.
[40] Chen J, Zhu Y, Huang M, Zhao L, Liang S, Li Z. Study on hydrogen-affected interaction between dislocation and grain boundary by MD simulation. Comp Mater Sci 2021;196:110562.
[41] Yu H, Cocks A, Tarleton E. Discrete dislocation plasticity HELPs understand hydrogen effects in bcc materials. J Mech Phys Solids 2019;123:41–60.
[42] Itakura M, Kaburaki H, Yamaguchi M, Okita T. The effect of hydrogen atoms on the screw dislocation mobility in bcc iron: a first-principles study. Acta Mater 2013;61:6857–67.
[43] Oh C, Kim N, Kim Y, Baek J, Kim Y, Kim W. A finite element ductile failure simulation method using stress-modified fracture strain model. Eng Fract Mech 2011;78:124–37.
[44] Colombo C, Zafra García A, Belzunce J, Fernandez Pariente I. Sensitivity to hydrogen embrittlement of AISI 4140 steel: a numerical study on fracture toughness. Theor Appl Fract Mech 2020;110:102810.

[45] Jiang DE, Carter EA. First principles assessment of ideal fracture energies of materials with mobile impurities: implications for hydrogen embrittlement of metals. Acta Mater 2004;52:4801–7.
[46] Kim J, Kim Y, Lee M, Kim K, Shibanuma K. Fracture simulation model for API X80 Charpy test in Ductile-Brittle transition temperatures. Int J Mech Sci 2020;182:105771.
[47] Wasim M, Djukic MB. Hydrogen embrittlement of low carbon structural steel at macro-, micro- and nano-levels. Int J Hydrogen Energy 2020;45:2145–56.
[48] Dong X, Wang D, Thoudden-Sukumar P, Tehranchi A, Ponge D, Sun B, et al. Hydrogen-associated decohesion and localized plasticity in a high-Mn and high-Al two-phase lightweight steel. Acta Mater 2022:118296.
[49] Djukic MB, Sijacki Zeravcic V, Bakic GM, Sedmak A, Rajicic B. Hydrogen damage of steels: a case study and hydrogen embrittlement model. Eng Fail Anal 2015;58:485–98.
[50] Martin ML, Fenske JA, Liu GS, Sofronis P, Robertson IM. On the formation and nature of quasi-cleavage fracture surfaces in hydrogen embrittled steels. Acta Mater 2011;59:1601–6.
[51] Nagao A, Smith CD, Dadfarnia M, Sofronis P, Robertson IM. The role of hydrogen in hydrogen embrittlement fracture of lath martensitic steel. Acta Mater 2012;60:5182–9.
[52] Wang S, Martin ML, Sofronis P, Ohnuki S, Hashimoto N, Robertson IM. Hydrogen-induced intergranular failure of iron. Acta Mater 2014;69:275–82.
[53] Huang C, Gao X. Phase field modeling of hydrogen embrittlement. Int J Hydrogen Energy 2020;45:20053–68.
[54] Alvaro A, Olden V, Akselsen OM. 3D cohesive modelling of hydrogen embrittlement in the heat affected zone of an X70 pipeline steel – Part II. Int J Hydrogen Energy 2014;39:3528–41.
[55] Meng B, Gu C, Zhang L, Zhou C, Li X, Zhao Y, et al. Hydrogen effects on X80 pipeline steel in high-pressure natural gas/hydrogen mixtures. Int J Hydrogen Energy 2017;42:7404–12.
[56] Nguyen TT, Heo HM, Park J, Nahm SH, Beak UB. Damage assessment and mechanical performance of Cr-Mo steel used in hydrogen storage vessels. Eng Fail Anal 2021;120:105031.
[57] Hüter C, Shanthraj P, McEniry E, Spatschek R, Hickel T, Tehranchi A, et al. Multiscale modelling of hydrogen transport and segregation in polycrystalline steels. Metals 2018;8(6):430.
[58] Deng Y, Barnoush A. Hydrogen embrittlement revealed via novel in situ fracture experiments using notched micro-cantilever specimens. Acta Mater 2018;142:236–47.
[59] Rogne BRS, Kheradmand N, Deng Y, Barnoush A. In situ micromechanical testing in environmental scanning electron microscope: a new insight into hydrogen-assisted cracking. Acta Mater 2018;144:257–68.
[60] Iijima T, Itoga H, An B, San Marchi C, Somerday BP. Measurement of fracture properties for ferritic steel in high-pressure hydrogen gas. In: Pressure vessels and piping conference, vol. 46049. American Society of Mechanical Engineers; 2014.
[61] Ma K, Peng W, Zheng J, Gu C, Zhang R, Liu Y, et al. Study on fracture strain of Cr–Mo steel in high pressure hydrogen. Int J Hydrogen Energy 2021;46:31501–9.
[62] Zafra A, Belzunce J, Rodríguez C. Hydrogen diffusion and trapping in 42CrMo4 quenched and tempered steel: influence of quenching temperature and plastic deformation. Mater Chem Phys 2020;255:123599.
[63] Hua Z, Zhang X, Zheng J, Gu C, Cui T, Zhao Y, et al. Hydrogen-enhanced fatigue life analysis of Cr–Mo steel high-pressure vessels. Int J Hydrogen Energy 2017;42:12005–14.
[64] Cui TC, Liu PF, Gu CH. Finite element analysis of hydrogen diffusion/plasticity coupled behaviors of low-alloy ferritic steel at large strain. Int J Hydrogen Energy 2017;42:20324–35.
[65] Ma K, Zheng J, Hua Z, Gu C, Zhang R, Liu Y. Hydrogen assisted fatigue life of Cr–Mo steel pressure vessel with coplanar cracks based on fatigue crack growth analysis. Int J Hydrogen Energy 2020;45:20132–41.
[66] Serebrinsky S, Carter EA, Ortiz M. A quantum-mechanically informed continuum model of hydrogen embrittlement. J Mech Phys Solids 2004;52:2403–30.
[67] Nibur KA, San Marchi C, Somerday BP. Fracture and fatigue tolerant steel pressure vessels for gaseous hydrogen. Pressure Vessels and Piping Conference 2010;49255. 2010.
[68] Dadfarnia M, Nibur KA, San Marchi CW, Sofronis P, Somerday BP, Foulk IJW, et al. Measurement and interpretation of threshold stress intensity factors for steels in high-pressure hydrogen gas. Albuquerque, NM, and Livermore, CA (United States): Sandia National Laboratories (SNL); 2010. No. SAND2010-4633.
[69] Gu C, Yao Y, Zhao Y, Ma K, Kuang J, Zhang R, et al. Experimental study on fracture mechanical properties of 4130X in 50 MPa hydrogen environment. Light Industry Machinery 2021;39:8–13.
[70] Wang M, Akiyama E, Tsuzaki K. Effect of hydrogen and stress concentration on the notch tensile strength of AISI 4135 steel. Mater Sci Eng, A 2005;398:37–46.
[71] Olden V, Thaulow C, Johnsen R, Østby E, Berstad T. Influence of hydrogen from cathodic protection on the fracture susceptibility of 25%Cr duplex stainless steel – constant load SENT testing and FE-modelling using hydrogen influenced cohesive zone elements. Eng Fract Mech 2009;76:827–44.
[72] Thomas RLS, Scully JR, Gangloff RP. Internal hydrogen embrittlement of ultrahigh-strength AERMET 100 steel. Metall Mater Trans 2003;34:327–44.
[73] Zhai J, Shang X, Wang H, Xu T, Yu H, Sun Y, et al. High-pressure hydrogen embrittlement evaluation method Research based on 4130X. Material. Materials Reports 2021;35:437–42.
[74] Nagumo M. Characteristic features of deformation and fracture in hydrogen embrittlement. In: Nagumo M, editor. Fundamentals of hydrogen embrittlement. Singapore: Springer Singapore; 2016. p. 137–65.